

# Evolution of broad emission lines from double-peaked to single-peaked to support a central tidal disruption event

XueGuang Zhang

Guangxi Key Laboratory for Relativistic Astrophysics, School of Physical Science and Technology, GuangXi University, Nanning, 530004, P. R. China e-mail: xgzhang@gxu.edu.cn

May 22, 2025

## ABSTRACT

In this manuscript, considering evolution of fallback accreting debris in a central Tidal Disruption Event (TDE), the outer boundary increased with time of the disk-like broad emission line regions (BLRs) lying into central accretion disk will lead expected broad emission lines changed from double-peaked to single-peaked. Considering common elliptical orbitals for the accreting fallback TDEs debris, based on simulated results through the preferred standard elliptical accretion disk model, a probability about 3.95% can be estimated for cases with double-peaked profile changed to single-peaked profile in multi-epoch broad emission lines, indicating such unique profile variability could be indicator for BLRs related to TDE debris. Meanwhile, among the reported optical TDE candidates with apparent broad lines, such profile changes in broad H $\alpha$  can be found in the AT 2018hyz. After accepted the outer boundaries of the disk-like BLRs increased with time, the observed multi-epoch broad H $\alpha$  can be described in AT 2018hyz. Moreover, the elliptical accretion disk model determined time dependent ratios of the outer boundaries of the disk-like BLRs are well consistent with the TDE model expected ratios of the outer boundaries of the fallback TDE debris. Furthermore, the evolution properties of disk-like BLRs can be applied to estimate the locations of the disk-like BLRs of which outer boundary could be about one sixth of the outer boundary of the fallback TDE debris in AT 2018hyz. Such unique profile changes from double-peaked to single-peaked could be applied as further clues to support a central TDE.

**Key words.** galaxies:active - galaxies:nuclei - galaxies:emission lines - transients:tidal disruption events

## 1. Introduction

Broad emission lines can be detected in optical spectrum in a Tidal Disruption Event (TDE), due to expected broad emission line regions (BLRs) lying into central accretion disk related to fallback TDE debris, as detailed discussions in Guillochon et al. (2014). Moreover, such disk-like BLRs lying into central accretion disk can commonly lead to double-peaked broad emission lines, as detailed discussions on accretion disk model in Chen et al. (1989); Chen & Halpern (1989); Eracleous et al. (1995); Storchi-Bergmann et al. (2003); Flohic & Eracleous (2008), etc. The model expected double-peaked broad emission lines have been reported in more than 400 broad line Active Galactic Nuclei (AGN), as reported results in Eracleous & Halpern (1994); Strateva et al. (2003); Zhang (2022, 2023); Ward et al. (2024); Zhang (2024b), etc. Meanwhile, there are some reports on double-peaked broad emission lines in TDE candidates, such as the discussed results in Yang et al. (2013); Liu et al. (2017); Hung et al. (2020); Short et al. (2020); Zhang (2021); Short et al. (2023); Ridley et al. (2024); Zhang (2024a), etc. However, there are different causes leading to variability of the double-peaked broad emission lines in AGN and in TDE candidates.

The unique disk-like structures of BLRs lying into central accretion disks can lead to unique time-dependent variability properties of the corresponding broad emission lines, commonly due to rotating motions in the disk-like BLRs, especially in broad line AGN. Storchi-Bergmann et al. (2003); Schimoia et al. (2012) have shown such variability of the double-peaked broad H $\alpha$  in the known NGC1097 by rotating disk-like BLRs lying into

central accretion disk. Similar variability properties of double-peaked broad emission lines can also be found in Gezari et al. (2007) and in Lewis et al. (2010) in small samples of broad line AGN.

Although there are similar accretion disk origin for the reported double-peaked broad emission lines in normal broad line AGN and in TDE candidates, one main difference should be noted between the physical properties of the corresponding BLRs in normal broad line AGN and in TDE candidates. As the discussed TDE candidates in Gezari (2021) and the more recent reported TDE candidates in Yao et al. (2023), the time durations of TDE candidates are around 1yr (mean values for the cases shown in Fig. 9 in Yao et al. 2023), very smaller than the variability time scale in double-peaked broad lines in AGN as shown in Storchi-Bergmann et al. (2003); Gezari et al. (2007); Lewis et al. (2010). The shorter time durations of TDE candidates probably indicate few effects of rotations in disk-like BLRs in TDE candidates on the corresponding broad lines. However, when considering the BLRs related TDE debris, the boundaries of the disk-like BLRs should increase with time, due to the time dependent evolution of fallback TDE debris, such as the shown results in Guillochon et al. (2014) for the outer boundary of TDE debris after considering the dimensionless evolution time  $t = T/T_0$  with  $T_0 = 2\pi(\frac{R_p^3}{G M_{BH}})^{1/2}$  ( $R_p$  as the pericenter distance) and  $T$  as the orbital period at radius different from  $R_p$  (such as in Lodato et al. 2011)

$$R_{tde,out} \sim 2\left(\frac{G M_{BH} t^2}{\pi^2}\right)^{1/3} \quad (1)$$

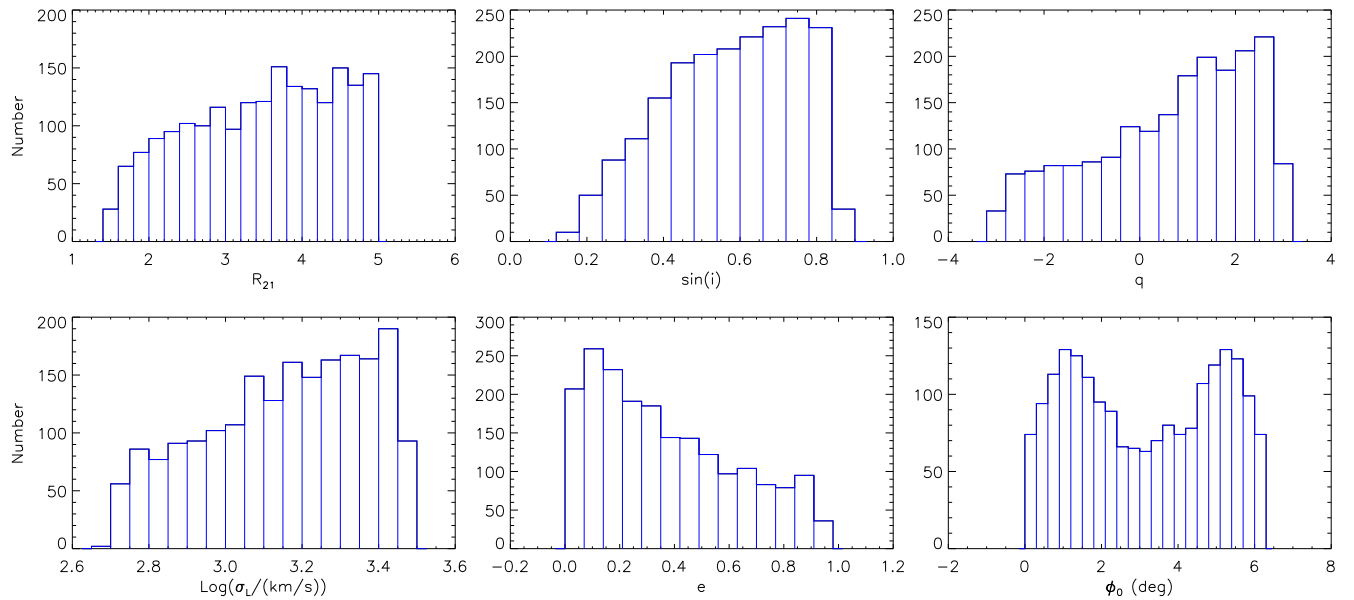


**Fig. 1.** Distributions of the model parameters of the 1977 cases which have profiles changed from double-peaked to single-leaked.

with  $M_{BH}$  and  $G$  as the central black hole (BH) mass and the Gravitational constant. Therefore, not similar as the commonly known disk-like BLRs in normal broad line AGN, the variability in line profiles of the broad lines from the disk-like BLRs in TDE candidates is not due to rotations, but probably mainly due to the variability of the outer boundary of the disk-like BLRs. To check the effects of the time dependent variability of outer boundary of the disk-like BLRs in TDE candidates is the main objective of this manuscript. Here, we should note that starting from evolution of outer radius of disk-like BLRs in TDEs, line profile variability of double-peaked broad lines are mainly considered in our manuscript, not to determine physical origin of line profile variability of double-peaked broad lines.

This manuscript is organized as follows. Section 2 presents our main results through the elliptical accretion disk model (Eracleous et al. 1995) and necessary discussions on variability properties of double-peaked broad lines due to variability of outer boundary of the disk-like BLRs in TDE candidates. Section 3 shows discussions on another explanations to the changed profiles of broad emission lines. Section 4 gives our main summary and conclusions. And in this manuscript, we have adopted the cosmological parameters of  $H_0 = 70 \text{ km} \cdot \text{s}^{-1} \text{Mpc}^{-1}$ ,  $\Omega_\Lambda = 0.7$  and  $\Omega_m = 0.3$ .

## 2. Main results

In this manuscript, the elliptical accretion disk model proposed in Eracleous et al. (1995) is accepted to describe expected double-peaked broad emission lines from disk-like BLRs lying into central accretion disk. There are seven free model parameters, the inner boundary  $R_{in}$  (in units of  $R_G$  with  $R_G$  as the Schwarzschild radius) and the outer boundary  $R_{out}$  (in units of  $R_G$ ) of the disk-like emission regions, the eccentricity  $e$  of the emission regions, the inclination angle  $i$  of the emission regions, the line emissivity power-law index  $f_r \propto r^{-q}$ , the local turbulent broadening velocity  $\sigma_L$  (in units of km/s), and the orientation angle  $\phi_0$ . Here, the improved circular accretion disk plus spiral arms model (Storchi-Bergmann et al. 2003) is not considered, mainly due to the following reason. As discussed in Guillochon et al. (2014), the fallback TDE debris are commonly in elliptical or

**Table 1.** Model parameters for the elliptical accretion disk model

par	units	model	Elli
$R_{in}$	$R_G$	[100, 600]	$166 \pm 90$
$R_{out}$	$R_G$	$k_0 \times R_{in}$ ( $k_0 \in [1.5, 5]$ )	$880 \pm 113$
$R_{out2}$	$R_G$	$k \times R_{out}$ ( $k \in [1.5, 5]$ )	$1006 \pm 260$
	$R_G$		$1236 \pm 370$
	$R_G$		$1340 \pm 502$
	$R_G$		$1900 \pm 764$
$\sin(i)$		[0.3, 0.9]	$0.62 \pm 0.03$
$q$		[-3, 3]	$-0.103 \pm 0.687$
$e$		[0, 0.95]	$0.133 \pm 0.018$
$\sigma_L$	km/s	[500, 3000]	$1893 \pm 200$
	km/s		$750 \pm 164$
	km/s		$1720 \pm 220$
	km/s		$1818 \pm 198$
	km/s		$2515 \pm 357$
$\phi_0$	rad	[0, $2\pi$ ]	$0.12 \pm 0.04$

Notice: The first column and the second column show the applied model parameters and the corresponding units. The third column shows the limited range ([lower boundary, upper boundary]) of each model parameter in the elliptical accretion disk model leading to the artificial  $f_{A1}$  and  $f_{A2}$ . The fourth column shows the determined model parameters in the elliptical accretion disk model applied to describe the time dependent line profiles of broad H $\alpha$  in AT 2018hyz. In the fourth column, the five values in  $R_{out}$  and  $R_{out2}$  and the five values in  $\sigma_L$  are for the five broad H $\alpha$  with  $\Delta t = 17, 51, 117, 120, 164$  days.

bits, such as the shown results in Fig. 2 in Guillochon et al. (2014), therefore, the standard elliptical accretion disk model discussed in Eracleous et al. (1995) is mainly considered. Simple discussions on the circular accretion disk plus spiral arms model (Storchi-Bergmann et al. 2003) should be given in the following Section 3.

Based on the elliptical accretion disk model, the first thing we should do is to estimate a probability to detect the profile change from double-peaked to single-peaked due to increased outer boundary  $R_{out}$  with time. The following procedures are ap-

plied. For the first step, the seven model parameters are randomly collected within the limited ranges listed in Table 1, leading to a model created line profile  $f_{\lambda 1}$ . Here, the model parameter  $R_{out}$  is collected by  $k_0 \times R_{in}$  with  $k_0$  as a random value from 1.5 to 5. And the listed range for each model parameter is common, see results in Strateva et al. (2003). For the second step, a new value of the outer boundary  $R_{out2}$  is randomly collected by  $R_{out2} \sim k \times R_{out}$  ( $k$  as a random value from 1.5 to 5) with  $R_{out}$  as the value collected in the first step, leading to the new model created line profile  $f_{\lambda 2}$  with different outer boundaries but with the same values for the other model parameters. For the third step, if  $f_{\lambda 1}$  has more than two peaks but  $f_{\lambda 2}$  has only one peak, we accept the case is the one which has the changed profile from double-peaked to single-peaked. Here, the function `find_peaks` (included in the package `idlspc2d` with version 5.2.0 in Sloan Digital Sky Survey) is applied to detect peaks in line profiles. Then, to repeat the three above steps 50000 times, there are 1977 cases having the changed profiles from the double-peaked to single-peaked. Although the model created cases are oversimplified, the results indicate the probability roughly about 3.95% (1977/50000) to detect changed profiles in multi-epoch optical spectrum, assumed that the outer boundaries of the disk-like BLRs in TDE candidates are increased with time. Moreover, based on the dynamical properties of the emission clouds in disk-like BLRs, the full width at zero intensity of the broad emission line sensitively depends on the inner boundary of the disk-like BLRs, but the peak separation of the broad emission line sensitively depends on the outer boundary. Larger outer boundary leads to smaller peak separation of the double-peaked broad emission line. Once the peak separation is smaller enough, single-peaked rather than apparent double-peaked broad emission line could be expected from disk-like BLRs.

Here, we should note that our main objective to do the simulation is to check a probability for TDE expected evolution of outer radius of disk-like BLRs leading double-peaked broad emission line to be changed to single-peaked. Now, based on the randomly collected model parameters within reasonable limited ranges, a not very low probability about 3%-4% can be obtained, indicating among the reported more than 300 optical TDEs, there should be several TDEs which could have changed line profiles in their broad emission lines as expected by the simulations. Therefore, it is the basic point to support us in doing the following work in the manuscript. Unfortunately, through randomly collected model parameters in reasonable parameter space vast enough, if the corresponding simulations can not lead to an acceptable probability, it is very hard at current stage for us to find a more optimized way to determine a more trustworthy probability.

Based on the simulated results, Fig. 1 shows the distributions of the parameters of  $R_{21} = \frac{R_{out2}}{R_{out}}$ ,  $\sin(i)$ ,  $q$ ,  $\sigma_L$ ,  $e$  and  $\phi_0$  of the 1977 cases. It is clear that the detected changed profile from double-peaked to single-peaked has not sensitively dependence on the model parameters. Moreover, an example of expected line profile variability is shown in Fig. 2 by changing the model parameter of  $R_{out}$  but with the other model parameters to be fixed, leading the model expected double-peaked profile changed to single-peaked profile due to small  $R_{out}$  varied to large  $R_{out2}$ .

Before proceeding further, considering the changed line profile from double-peaked to single-peaked due to increases  $R_{out}$ , further clues could be obtained to support central TDE and/or to estimate locations of BLRs in TDE candidates. Accepted the time dependent evolution of  $R_{TDE,out}$  (shown in equation 1 in the Introduction) discussed in Guillochon et al. (2014), If there were clear time information for the double-peaked line profile (at time

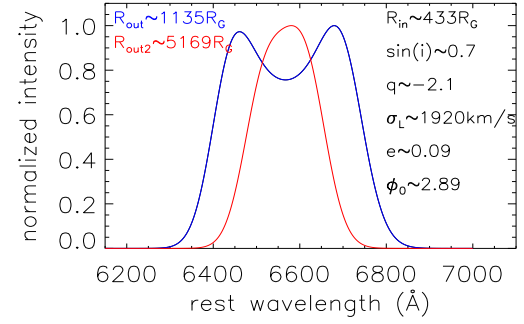


**Fig. 2.** An example on the broad H $\alpha$  with double-peaked profile (in blue) expected by the elliptical accretion disk model with smaller  $R_{out}$ , but with single-peaked profile (in red) expected by the model with larger  $R_{out2}$ . The applied model parameters, except the  $R_{out}$  and  $R_{out2}$  marked in the top left corner, are marked in the top right corner.

$t_d$ ) and the single-peaked line profile (at time  $t_s$ ), then through the  $t_d$  and  $t_s$  and the determined  $R_{out2}$ ,  $R_{out}$ , assumed the central disk-like BLRs have the similar expanded properties as the fallback TDE debris, we will have the following two sub-equations

$$\begin{aligned} \left(\frac{t_s}{t_d}\right)^{2/3} &\sim \frac{R_{out2}}{R_{out}} \\ 2\left(\frac{GM_{BH}t_s^2}{\pi^2}\right)^{1/3} - 2\left(\frac{GM_{BH}t_d^2}{\pi^2}\right)^{1/3} &\geq (R_{out2} - R_{out}) \end{aligned} \quad (2)$$

Therefore, the first sub-equation can be applied to test whether there are expected increased outer boundaries of the disk-like BLRs related to TDE debris. Meanwhile, considering  $R_{out}$  in units of  $R_G = \frac{GM_{BH}}{c^2}$  ( $c$  as the light speed), the second sub-equation above can be re-written as

$$\begin{aligned} Fr_t = t_s^{2/3} - t_d^{2/3} &= k_s \Delta R_{out} \times \frac{(GM_{BH}\pi)^{2/3}}{2c^2} \quad (k_s \geq 1) \\ \Delta R_{out} &= \frac{R_{out2}}{R_G} - \frac{R_{out}}{R_G} \end{aligned} \quad (3)$$

It is clear that the equation 3 can provide an independent method to estimate the locations of the disk-like BLRs in central accretion disk in an assumed TDE, if the central BH mass has been measured. For the equation 3, unless the disk-like BLRs and the fallback TDE debris have the same outer boundaries, the factor  $k_s = 1$  is preferred, otherwise  $k_s > 1$ .

Based on the model dependent results, it is interesting to check whether double-peaked broad lines changed to single-peaked can be detected in a real TDE candidate. Among the reported TDE candidates, there is one TDE candidate AT 2018hyz of which broad H $\alpha$  shows double-peaked features in the early stage but single-peaked features in the late stage. The detailed discussions on both the photometric variability and the spectroscopic properties can be found in Hung et al. (2020). Based on the collected data points binned with 4.5 Å from the Fig. 3 in Hung et al. (2020) for the spectra after subtractions of host galaxy contributions, the clear line profiles of the five broad H $\alpha$  with  $\Delta t \sim 27, 51, 117, 120, 164$  days ( $\Delta t$  as the time interval since the discovery at MJD=58432) are shown in the left panel of Fig 3. Here, we should note that the continuum emissions underneath the broad H $\alpha$  have been removed by a linear function determined by the data points with rest wavelength from 6200 Å to 6350 Å and from 6820 Å to 7000 Å. Meanwhile, due to broad

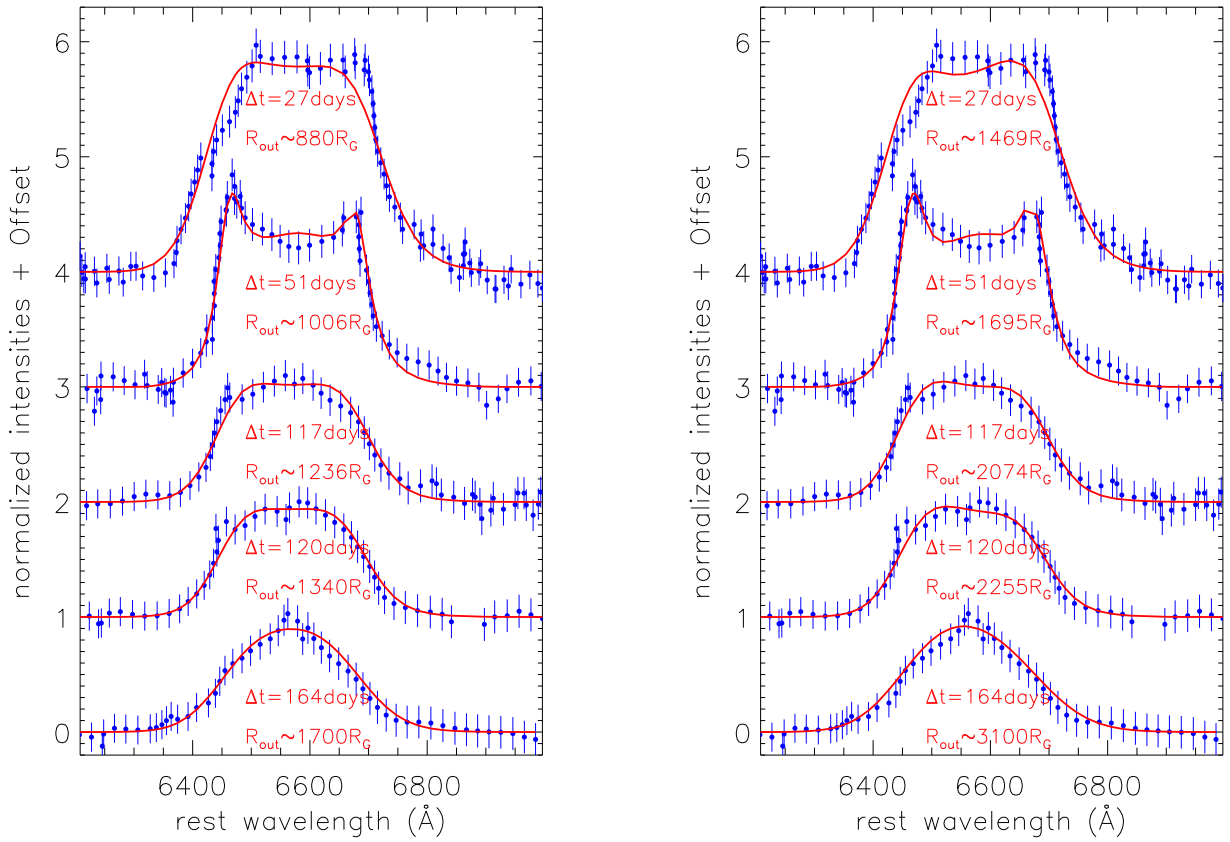


**Fig. 3.** Left panel shows the best descriptions (solid red lines) to the multi-epoch broad H $\alpha$  (solid circles plus error bars in blue) in AT 2018hyz by the elliptical accretion disk model. The corresponding  $\Delta t$  and outer boundary of the disk-like BLRs for each broad H $\alpha$  are marked as red characters. Right panel shows the corresponding results through the circular accretion disk plus spiral arms model.

H $\alpha$  not complete and/or due to no apparent broad features, the spectroscopic features around 6564 $\text{\AA}$  are not considered for the two spectra with  $\Delta t \sim 199, 364$  days. Clearly, the first two broad H $\alpha$  with  $\Delta t \sim 27, 51$  days have apparent double-peaked features. However, the other three broad H $\alpha$  with  $\Delta t \sim 117, 120, 164$  days have relatively smooth profiles without apparent double-peaked features.

Now, it is interesting to check whether considering the increased outer boundaries  $R_{out}$  can be applied to describe the profile variability in the five broad H $\alpha$  in AT 2018hyz. Here, the elliptical accretion disk model are applied to simultaneously describe the five broad H $\alpha$ , with the following model parameters. The five values of  $R_{out}$  are increased with time for the five broad H $\alpha$ . There are also five values of  $\sigma_L$  for the five broad H $\alpha$ . The varying  $\sigma_L$  can be commonly accepted, considering the evolution of disk-like BLRs covering different emission regions. Besides the  $R_{out}$  and  $\sigma_L$ , the other model parameters are the same for each broad H $\alpha$ , when to describe the broad H $\alpha$ . Therefore, when the model applied to describe the five broad H $\alpha$ , there are 15 model parameters,  $R_{in}$ , five  $R_{out}$ ,  $\sin(i)$ ,  $q$ ,  $e$ , five  $\sigma_L$  and  $\phi_0$ . Then through the Levenberg-Marquardt least-squares minimization technique (the MPFIT package) (Markwardt 2009), left panel of Fig. 3 shows the best descriptions to the five broad H $\alpha$ , with the corresponding  $\chi^2/dof \sim 1.05$  ( $dof$  as degree of freedom). The determined model parameters are listed in the fourth column in Table 1. The five values of  $R_{out}$  increased with time are also marked in the left panel of Fig. 3.

As discussed in Hung et al. (2020) through applications of theoretical TDE model Guillochon & Ramirez-Ruiz (2013); Guillochon et al. (2014); Mockler et al. (2019) to describe long-term photometric variability of AT 2018hyz, the time interval is about  $-43^{+8}_{-9}$  days between the starting time  $t_0$  for the assumed TDE and the time for the discovery of AT 2018hyz. Therefore, the corresponding time information in rest frame for the five observed broad H $\alpha$  since  $t_0$  are about  $t_1 = (27 + 43)^{+8}_{-9}$  days,  $t_2 = (51 + 43)^{+8}_{-9}$  days,  $t_3 = (117 + 43)^{+8}_{-9}$  days,  $t_4 = (120 + 43)^{+8}_{-9}$  days and  $t_5 = (164 + 43)^{+8}_{-9}$  days. Then, for any two of the broad H $\alpha$ , there are ten  $R_{out}$  ratios,  $R_{ij} = R_{out,t_i}/R_{out,t_j}$  ( $R_{out,t_i}$  as the determined  $R_{out}$  for the broad H $\alpha$  at  $t_i$ ) with  $t_i > t_j$ , and also corresponding ten time ratios,  $t_{ij} = t_i/t_j$  with  $t_i > t_j$ .

Top left panel of Fig. 4 shows the dependence of the ratio  $R_{ij}$  on the ratio  $t_{ij}^{2/3}$ , leading to a linear dependence as expected by the first sub-equation in equation 2. There are only ten data points, therefore, there are no further discussions on the robust of the linear dependence but to show the determined Spearman Rank correlation coefficient about 0.58 ( $P_{null} \sim 0.08$ ). Furthermore, top right panel of Fig. 4 shows the dependence of the  $R_{out}$  difference  $\Delta R_{ij} = R_{out,t_i} - R_{out,t_j}$  ( $t_i > t_j$ ) on the corresponding  $Fr_t$  with Spearman Rank correlation coefficient about 0.62 ( $P_{null} \sim 0.05$ ). Accepted the central BH mass  $3.5 \times 10^6 M_\odot$  in AT 2018hyz as discussed in Hung et al. (2020),  $k_s \sim 6.5$  applied in equation 3 can describe the shown dependence of  $\Delta R_{ij}$  on  $Fr_t$ . Therefore, the outer boundaries of the disk-BLRs for the broad

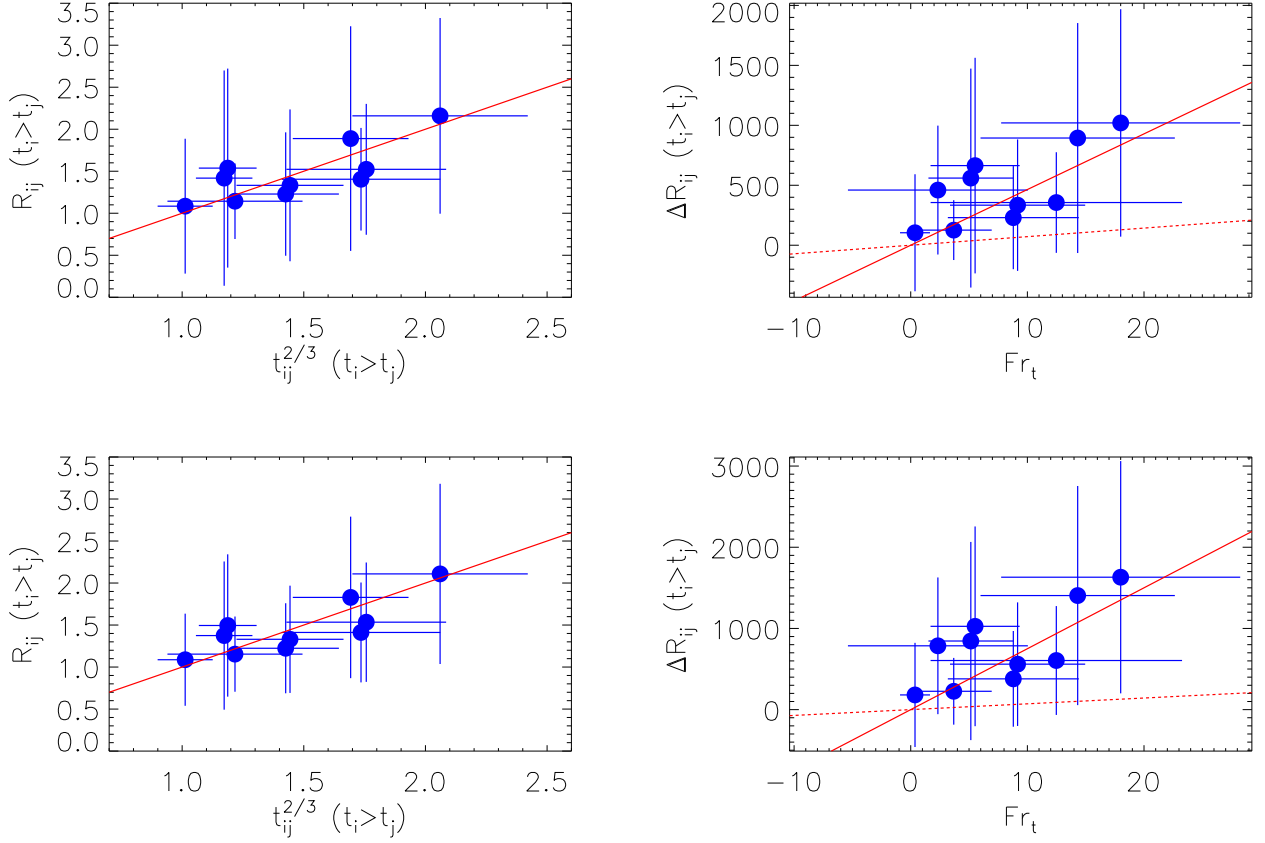


**Fig. 4.** Top left panel shows the dependence of  $R_{ij}$  on  $t_{ij}^{2/3}$ . Solid red line shows  $R_{ij} = t_{ij}^{2/3}$ , based on the determined parameters by the elliptical accretion disk model. Top right panel shows the dependence of  $\Delta R_{ij}$  on  $Fr_t$ , based on the determined parameters by the elliptical accretion disk model. In the top right panel, dashed red line and solid red line show the  $Fr_t = \Delta R_{ij} \frac{(GM_{BH}\pi)^{2/3}}{2c^2}$  and  $Fr_t = 6.5\Delta R_{ij} \frac{(GM_{BH}\pi)^{2/3}}{2c^2}$ , respectively. Bottom panels show the corresponding results based on the determined parameters by the circular accretion disk plus spiral arms model. In bottom left panel, solid red line shows  $R_{ij} = t_{ij}^{2/3}$ . In bottom right panel, dashed red line and solid red line show the  $Fr_t = \Delta R_{ij} \frac{(GM_{BH}\pi)^{2/3}}{2c^2}$  and  $Fr_t = 10.5\Delta R_{ij} \frac{(GM_{BH}\pi)^{2/3}}{2c^2}$ , respectively.

$H\alpha$  are about one sixth of the outer boundaries of the fallback TDEs debris in AT 2018hyz.

Before ending the section, three additional points are noted. For the first point, it is necessary to check whether disk rotating have strong effects on the profile variability of broad  $H\alpha$  in AT 2018hyz. Based on the determined eccentricity, inner and outer boundaries of the disk-like BLRs, the expected disk precession period as discussed in Storchi-Bergmann et al. (2003) is about  $T_{pre}$

$$T_{pre} \sim 10.4M_{BH,6} \frac{1+e}{(1-e)^{3/2}} R_{em,3} \text{ yrs} \quad (4)$$

with  $M_{BH,6}$  as the BH mass in units of  $10^6 M_\odot$  and  $R_{em,3}$  as the distance in units of  $10^3 R_G$  of disk-like BLRs to central BH and  $e$  as the eccentricity of the disk-like BLRs. For AT 2018hyz,  $M_{BH,6}$  is about 3.5,  $e \sim 0.133$ , and the  $R_{em,3}$  can be estimated to be 0.612 by the flux-weighted distance from central BH after considering the model parameters in the elliptical accretion disk model to describe the broad  $H\alpha$  with  $\Delta t = 17$  days. Therefore, the expected disk precession period is about 15 years, very longer than the time intervals only around 150 days for the broad  $H\alpha$  in AT 2018hyz. Moreover considering the model parameters for the

other broad  $H\alpha$ , due to larger outer boundary, longer procession period than 15 years can be expected. Therefore, there are few effects of disk procession on profile variability of broad  $H\alpha$  in AT 2018hyz. For the second point, the listed model parameters are not similar as the ones reported in Hung et al. (2020), mainly due to no considerations of extra Gaussian components in the broad  $H\alpha$  in this manuscript. Therefore, there are no further discussions on different model parameters in this manuscript and in Hung et al. (2020). For the third point, the determined  $\sigma_L$  at  $\Delta t = 51$  days is very different from the  $\sigma_L$  at the other epochs, probably due to different local temperatures. As the shown Fig. 8 in Mockler et al. (2019), after the peak, the temperature decreases slightly near peak and then gradually increases as the luminosity decreases for common TDE candidates. Therefore, in AT 2018hyz, the expected temperature at  $\Delta t = 51$  days should be the minimum value, leading to the smaller temperature dependent  $\sigma_L$ .

Before ending the section, there is one point we should note. In the accretion disk models above for the simulations, the corresponding boundaries of emission regions are in units of  $R_G$ , leading the simulations not to depend on BH masses or boundaries of BLRs in physical distance units, indicating the simulations can be commonly applied in BLRs related to any TDEs. In other words, the simulations are through the known accretion

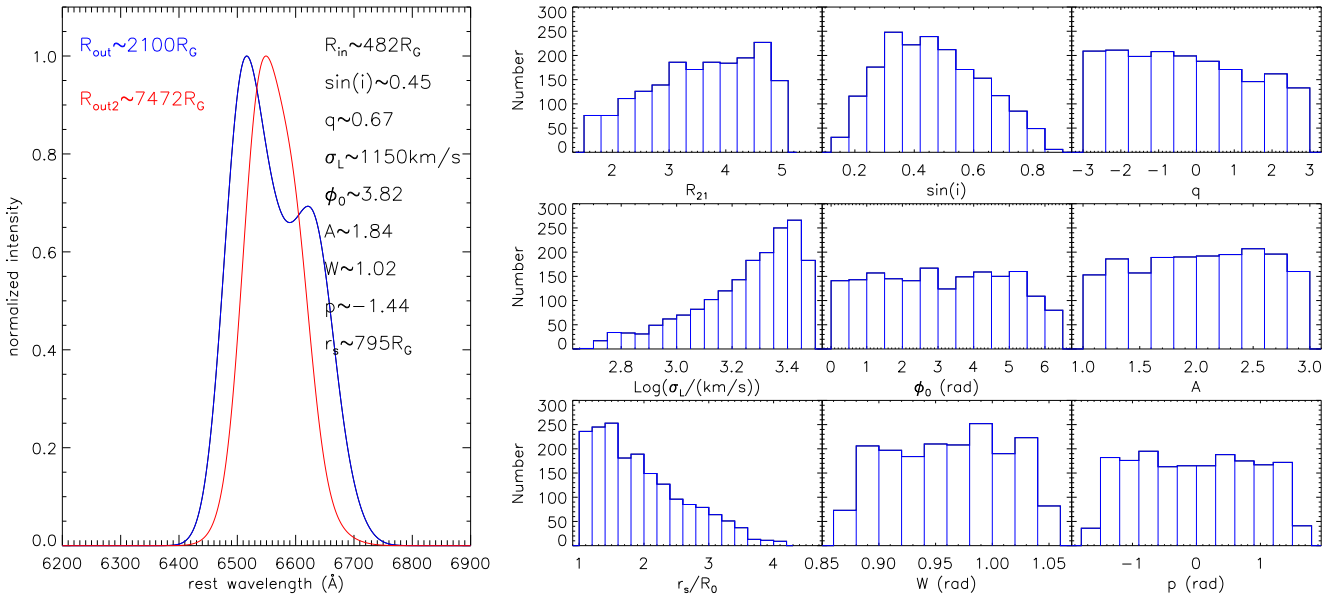


**Fig. 5.** Left panel shows an example on the broad H $\alpha$  with double-peaked profile (in blue) expected by the circular accretion disk plus spiral arms model with smaller  $R_{out}$ , but with single-peaked profile (in red) expected by the model with larger  $R_{out2}$ . The applied model parameters, except the  $R_{out}$  and  $R_{out2}$  marked in the top left corner, are marked in the top right corner. The other panels show the distributions of the model parameters of the 1825 cases which have profiles changed from double-peaked to single-peaked, through the circular accretion disk plus spiral arms model.

**Table 2.** Model parameters for the circular accretion disk plus spiral arms model

par	units	model	Arm
$R_{in}$	RG	[100, 600]	$268 \pm 170$
$R_{out}$	RG	$k_0 \times R_{in}$ ( $k_0 \in [1.5, 5]$ )	$1469 \pm 266$
$R_{out2}$	RG	$k \times R_{out}$ ( $k \in [1.5, 5]$ )	$1695 \pm 330$
	RG		$2074 \pm 470$
	RG		$2255 \pm 630$
	RG		$3100 \pm 950$
$\sin(i)$		[0.3, 0.9]	$0.69 \pm 0.05$
$q$		[-3, 3]	$-0.267 \pm 0.395$
$\sigma_L$	km/s	[500, 3000]	$1800 \pm 165$
	km/s		$700 \pm 100$
	km/s		$1788 \pm 235$
	km/s		$1877 \pm 207$
	km/s		$3000 \pm 337$
$\phi_0$	rad	[0, $2\pi$ ]	$1.87 \pm 0.63$
$A$		[1, 3]	$2.72 \pm 0.42$
$W$	degree	[10, 60]	$58 \pm 27$
$p$	degree	[-90, 90]	$33 \pm 10$
$r_s$	$R_G$	$[r_0, 0.8r_1]$	$270 \pm 160$

Notice: The first column and the second column show the applied model parameters and the corresponding units. The third column shows the limited range ([lower boundary, upper boundary]) of each model parameter in the elliptical accretion disk model leading to the artificial  $f_{\lambda 1}$  and  $f_{\lambda 2}$ . The fourth column shows the determined model parameters in the circular accretion disk plus spiral arms model applied to describe the time dependent line profiles of broad H $\alpha$  in AT 2018hyz. In the fourth column, the five values in  $R_{out}$  and  $R_{out2}$  and the five values in  $\sigma_L$  are for the five broad H $\alpha$  with  $\Delta t = 17, 51, 117, 120, 164$  days.

disk models, previously given BH masses and/or boundaries of BLRs have no effects on the corresponding simulation results, only except the  $r_{in}$  and  $r_{out}$  described in physical distance units

of light-days and/or pc and/or km. In one word, through the simulations by accretion disk models with or without given values of BH mass and/or boundaries of BLRs, the same results can be determined. Therefore, there are no discussions on effects of given BH mass and/or boundaries of BLRs in the manuscript.

### 3. Another explanations to the changed profiles of double-peaked broad emission lines

Considering the accreting fallback TDEs debris commonly in elliptical orbits as discussed in Guillochon et al. (2014), the elliptical accretion disk model is mainly considered and discussed above. However, there are several other explanations to the changed profiles of double-peaked emission lines related to disk-like BLRs. In the section, the following two additional explanations are mainly discussed.

Considering eccentricity of the disk-like BLRs to be zero, the improved circular disk plus spiral arms model (Storchi-Bergmann et al. 2003) is discussed with ten model parameters. Besides the model parameters (with eccentricity to be zero) applied in the elliptical accretion disk model (Eraclaeus et al. 1995), there are four addition parameters, the contrast ratio  $A$  for the arms relative to the rest of the disk, the width  $W$  and pitch angle  $p$  for the arms, and the starting radius  $r_s$  (in units of  $R_G$ ) of the arms. As an optional model to explain double-peaked broad lines, through dynamical properties of disk-like BLRs. It is obvious that larger outer boundary of the disk-like BLRs in the circular disk plus spiral arms model can also lead to smaller peak separation of double-peaked broad emission lines.

Similar as what we have done in Section 2 on the elliptical accretion disk model, the following procedure is applied based on the circular accretion disk plus spiral arms model. First, the ten model parameters are randomly collected within the limited ranges listed in Table 2, leading to a model created line profile  $f_{\lambda 1}$ . Second, a new value of the outer boundary  $R_{out2}$  is randomly collected by  $R_{out2} \sim k \times R_{out}$ , leading to the new model created line profile  $f_{\lambda 2}$  with different outer boundaries but with the same

values for the other model parameters. Third, if  $f_{\lambda 1}$  has more than two peaks but  $f_{\lambda 2}$  has only one peak, we accept the case is the one which has the changed profile from double-peaked to single-peaked through the circular accretion disk plus spiral arms model. Then, to repeat the three above steps 50000 times, there are 1825 cases having the changed profiles from double-peaked to single-peaked, indicating the probability roughly about 3.65% (1825/50000) to detect changed profiles in multi-epoch optical spectrum with considerations of the evolved outer boundaries of the disk-like BLRs in TDE candidates. Left panel of Fig. 5 shows an example on the broad  $H\alpha$  with double-peaked profile expected by the circular accretion disk plus spiral arms model with smaller  $R_{out}$ , but with single-peaked profile expected by the model with larger  $R_{out2}$ . The other panels of Fig. 5 show the distributions of the model parameters of the 1825 cases. Therefore, the circular accretion disk plus spiral arms model can also lead to broad line profiles changed from double-peaked to single-peaked.

Then, the circular accretion disk plus spiral arms model has been also applied to describe the variability of broad  $H\alpha$  in AT 2018hyz through the Levenberg-Marquardt least-squares minimization technique, the determined model parameters are listed in the last column of Table 2, and the best fitting results are shown in the right panel of Fig. 3 with the corresponding  $\chi^2/dof \sim 1.02$ . And then, based on the determined model parameters by the circular accretion disk plus spiral arms model, bottom panels of Fig. 4 show the corresponding dependence of the ratio  $R_{ij}$  on the ratio  $t_{ij}^{2/3}$ , and the dependence of the  $R_{out}$  difference  $\Delta R_{ij} = R_{out,t_i} - R_{out,t_j}$  ( $t_i > t_j$ ) on the corresponding  $Fr_t$ . Strong linear correlations can be found in the bottom panels, with the determined Spearman Rank correlation coefficients about 0.62 ( $P_{null} \sim 0.02$ ) and 0.72 ( $P_{null} \sim 0.05$ ) for the results shown in the bottom left panel and in the bottom right panel, respectively. Meanwhile, accepted the central BH mass  $3.5 \times 10^6 M_\odot$  in AT 2018hyz,  $k_s \sim 10.5$  applied in equation 3 can describe the shown dependence of  $\Delta R_{ij}$  on  $Fr_t$  in the bottom right panel of Fig. 4. Therefore, assumed the circular accretion disk plus spiral arms model preferred in AT 2018hyz, the outer boundaries of the disk-BLRs for the broad  $H\alpha$  are about one tenth of the outer boundaries of the fallback TDEs debris in AT 2018hyz.

Unfortunately, there is not enough evidence to confirm which disk model, the elliptical accretion disk model or the circular accretion disk plus arms model, is preferred in the TDE candidate AT 2018hyz. However, considering that the elliptical orbitals are common in accreting fallback TDEs debris, the results through the elliptical accretion disk model are preferred, but the results through the circular accretion disk plus arms model can be accepted as potentially supplementary results.

Besides the evolution of outer boundary of disk-like BLRs expected by evolution of TDEs debris, disk instability (such as sudden hot spots, and/or radiation driven radial outflows) could be also applied to describe the broad line profiles changed from double-peaked to single-peaked, such as the more recent work on line profile variability of broad Balmer emission lines in NGC 1566 in Ochmann et al. (2024) due to strong scale-height-dependent turbulence. In other words, double-peaked broad line coming from disk-like BLRs can be changed to single-peaked broad line, after considering an addition emission component related to disk instability at one epoch. As discussed and shown in Hung et al. (2020), besides the double-peaked emission component in broad  $H\alpha$ , the extra Gaussian component can be accepted as the additional emission component related to disk instability. The extra Gaussian component has its strength comparable to

the strength of the double-peaked emission component, see results in Fig. 6 and Fig. 8 in Hung et al. (2020), indicating that the emission strength of the extra emission component related to the disk instability should be comparable to the common disk emission strength. In other words, the emissions from the process related to the disk instability should lead to apparent sudden bursts at the epochs for the disk instability, leading to expected apparent sudden flares in the optical light curves. However, after checking the photometric light curves in AT 2018hyz (see Fig. 1 in Hung et al. 2020), the light curves are smooth enough. Therefore, the scenario on disk instability is not preferred to explain the changed profiles in broad  $H\alpha$  in AT 2018hyz. Probably, in the near future, in one TDE with apparent sudden bursts/flares in optical light curves, strong turbulence related to disk instability could have contributions to explain broad emission lines having changed line profiles.

Besides the evolution of outer boundary of disk-like BLRs expected by evolution of TDEs debris and the probable disk instability, fountain-like AGN feedback proposed in Wada et al. (2023) can also be applied to explain the line profile variability of broad emission lines. However, our main results are discussed in the physical framework of TDEs with time scales around tens to hundreds of days, which is very smaller than the time scale about 10 (or more) years for fountain-like AGN feedback leading to line profile variability of broad emission lines. Therefore, there are no further discussions on the proposed scenario in Wada et al. (2023) in our manuscript. Furthermore, as discussed in Ochmann et al. (2024), a low-optical-depth wind could lead to drift of broad line profiles. Therefore, considering the proposed scenarios in Wada et al. (2023); Ochmann et al. (2024) on contributions of both wind and turbulence, not only changed profile from double-peaked to single-peaked but drifted line profile can be expected through the evolutions of broad emission lines. In the near future, to detect such unique variability properties of broad line profiles will provide interesting clues to support existence of turbulence and/or wind in TDEs with un-smooth light curves. Meanwhile, variability in outer radius of BLRs could also be due to variability of ionization luminosity, as expected by the reverberation mapping technique determined R-L relation between radius of BLRs and central continuum luminosity (Kaspi et al. 2000; Bentz et al. 2013). However, considering the smooth decline trend in the AT 2018hyz, central continuum luminosity weaken with time should lead outer radius of the disk-like BLRs to decrease over time, indicating more apparent double-peaked features. Therefore, the variability of outer radius by R-L empirical relation is not preferred in the AT 2018hyz. In the near future, to determine detailed time dependent spatial structures of disk-like BLRs through the known GRAVITY interferometric technique (Gravity Collaboration et al. 2018, 2021, 2024) in such TDEs with changed profiles of broad emission lines will provide further clues to support or to be against our proposed scenario in the manuscript.

## 4. Summary and Conclusions

The final summary and conclusions are as follows.

- Not similar as rotations in disk-like BLRs lying into central accretion disk leading to profile variability in broad line AGN, evolutions of outer boundaries of disk-like BLRs related to TDE debris can also lead profile variability of broad emission lines, especially lead to changed profile from double-peaked to single-peaked.
- Based on simulated results by standard elliptical accretion disk model preferred after considering elliptical orbitals for

accreting fallback TDEs debris, the probability is about 3.95% to detected profile changed from double-peaked to single-peaked in multi-epoch broad emission lines.

- Double-peaked broad H $\alpha$  in early stages but single-peaked broad H $\alpha$  can be detected in the TDE candidate AT 2018hyz.
- Only considering increased outer boundaries of the disk-like BLRs can lead to well accepted descriptions to profiles of the multi-epoch broad H $\alpha$  in AT 2018hyz.
- The dependence of outer boundary ratio  $R_{ij}$  on time interval ratio  $t_{ij}$  is well consistent with expected results by the evolution properties of fallback TDE debris in AT 2018hyz.
- Through the dependence of outer boundary difference  $\Delta R_{ij}$  on evolution time ratio  $Fr_t$ , outer boundary of the fallback TDE debris is about 6.5times of the outer boundary of the disk-like BLRs lying into central accretion disk in AT 2018hyz.
- Although the elliptical accretion disk model is preferred for the broad H $\alpha$  in the TDE AT 2018hyz, results on the improved circular accretion disk plus spiral arms model are also checked and discussed, indicating the outer boundary of the fallback TDE debris is about 10.5times of the outer boundary of the disk-like BLRs lying into central accretion disk in AT 2018hyz.
- Beside the accretion disk origin for the broad H $\alpha$ , disk instability can also be applied to explain the changed profiles of broad emission lines. However, applications of disk instability can lead to expected optical flares in photometric light curves. After considering the smooth photometric light curves in AT 2018hyz, the disk instability is not preferred to explain the changed profiles of broad H $\alpha$  in AT 2018hyz.
- Such unique profile variability in broad lines from double-peaked to single-peaked could be accepted as further clues to support a central TDE, besides the commonly applied photometric variability properties.

*Acknowledgements.* Zhang gratefully acknowledge the anonymous referee for giving us constructive comments and suggestions to greatly improve the paper. Zhang gratefully thanks the kind financial support from GuangXi University and the kind grant support from NSFC-12173020 and NSFC-12373014, and the support from Guangxi Talent Programme (Highland of Innovation Talents). This manuscript has made use of the MPFIT package (<http://cow.physics.wisc.edu/~craigm/idl/idl.html>).

## References

Bentz M. C., Denney, K. D.; Grier, C. J.; et al., 2013, ApJ, 767, 149  
 Chen, K.; Halpern, J. P.; Filippenko, A. V., 1989, ApJ, 339, 742  
 Chen, K.; Halpern, J. P., 1989, ApJ, 344, 115  
 Eracleous, M.; Halpern, J. P., 1994, ApJS, 90, 1  
 Eracleous, M.; Livio, M.; Halpern, J. P.; Storchi-Bergmann, T., 1995, ApJ, 438, 610  
 Flohic, H. M. L. G.; Eracleous, M., 2008, ApJ, 686, 138  
 Gezari, S.; Halpern, J. P.; Eracleous, M., 2007, ApJS, 169, 167  
 Gezari S., 2021, ARA&A, 59, 21  
 Gravity Collaboration; Sturm, E.; Dexter, J.; et al., 2018, Nature, 563, 657  
 GRAVITY Collaboration; Amorim, A.; Baubock, M.; et al., 2021, A&A, 648, 117  
 GRAVITY Collaboration; Amorim, A.; Bourdarot, G.; et al., 2024, A&A, 684, 167  
 Guillochon, J.; Ramirez-Ruiz, E., 2013, ApJ, 767, 25  
 Guillochon, J.; Manukian, H.; Ramirez-Ruiz, E., 2014, ApJ, 783, 23  
 Hung, T.; Foley, R. J.; Ramirez-Ruiz, E.; et al., 2020, ApJ, 903, 31  
 Kaspi, S., Smith, P. S., Netzer, H., Maoz, D., Jannuzi, B. T., Giveon, U., 2000, ApJ, 533, 631  
 Lewis, K. T.; Eracleous, M.; Storchi-Bergmann, T., 2010, ApJS, 187, 416  
 Liu, F. K.; Zhou, Z. Q.; Cao, R.; Ho, L. C.; Komossa, S., 2017, MNRAS Letter, 472, 99  
 Lodato, G.; King, A. R.; Pringle, J. E., 2011, MNRAS, 392, 332  
 Markwardt, C. B., 2009, ASPC, 411, 251  
 Mockler, B.; Guillochon, J.; Ramirez-Ruiz, E., 2019, ApJ, 872, 151